Identifying Reaction Pathway for Tandem Condensation-Hydrogenation to Produce Tetrahydroquinolines Using High-Pressure *Operando* NMR

Affiliations

Key words: tetrahydroquinolines, tandem catalysis, metal-organic frameworks, *operando* spectroscopy, mechanistic study.

Abstract

The sustainable synthesis of tetrahydroquinolines has been achieved by a bifunctional catalyst (Pd@UiO-66) driven Claisen-Schmidt condensation followed with a reductive intramolecular cyclization reaction. The one-pot tandem reactions with easily accessible precursors, 2-nitrobenzaldehyde and acetophenone, can be achieved with quantitative conversion. The high selectivity towards tetrahydroquinoline over quinoline has been substantiated *via* the mechanistic insights enabled by *operando* MAS-NMR spectroscopy with 400 psi H_2. Several reaction intermediates were identified, especially with the observation and quantification of reactive 2-phenyl-3,4-dihydroquinoline, which cannot be achieved with routine chromatographic techniques. The most probable reaction network was further deduced based on kinetics of intermediates and products. The procedure can be applied to acetophenone derivatives as building blocks carrying functional groups opening up other opportunities.

Introduction

1,2,3,4-Tetrahydroquinolines (THQs) architectures widely exist in bioactive natural products,[1] serving as hydrogen-storage materials and building blocks for the synthesis of key pharmaceutical ingredients, fragrance, and dyes.[2] The 2-substituted-THQs,[3] especially the 2-phenyl analogue (PTHQ), have attracted great interest as they can serve as platforms for the synthesis of reagents for the treatment of estrogen responsive cancer and osteoporosis.[4] Therefore, numerous protocols have been developed for the preparation of PTHQ,[1,5] and the most commonly employed method is the hydrogenation of quinolines with different catalysts.[6] Other approaches involve ring cyclization, including the intramolecular reductive cyclization of *ortho*-nitrochalcones, oxidative cyclization of amino alcohols,[7] intramolecular C–N bond formation of aryl azides,[8] and intermolecular atom-transfer radical addition (ATRA) followed by the intramolecular cyclization reaction.[9] However, the tedious synthetic procedures for the complex starting materials under harsh reaction conditions significantly restrict the further applications of these methods. Alternative methods were developed with more accessible substrates, particularly 2-nitrobenzaldehydes and enolizable ketones.[10] However, a two-step synthesis in a chlorinated solvent is still needed with more than one work-up procedure to isolate *ortho*-nitrochalcone intermediate. Therefore, a bifunctional catalyst to achieve both C-C bond formation and cyclization is highly desirable starting with readily available starting materials.

Scheme 1. Overview of previous and current work on the preparation of PTHQ.

Here, we constructed a bifunctional catalyst with Pd nanoparticles (NPs) supported on acidic MOF (UiO-66), so the formation of PTHQ from 2-nitrobenzaldehyde (NBA) and acetophenone (ACP) can be achieved in one-pot by sequential Claisen-Schmidt condensation and reductive intramolecular cyclization reaction. The transformation possibly involves multiple transiently-evolved intermediates as a result of partial reduction of several functionalities (i.e., NO_2, C=C, C=O, C=N, and arenes) before or after the ring formation. Understanding the evolution of the reaction network composed of the reaction intermediates is critical in directing the species distribution towards the desired product. The first step of such efforts is to deconvolute individual reaction paths and their reversibility. One of the examples is that the identification of a key intermediate during acid-catalyzed dehydration of fructose shows the limitation of the ultimate reaction optimization as the intermediate downflows to both the favored and unfavored reaction paths.[11] However, due to the co-presence of solid catalyst, reaction solution, and hydrogen gas, the molecular-level understanding is rather challenging to be probed, in particular when intermediate is not stable upon sampling. Even for stable species, the number of intermittent sampling greatly restricts the density of data points to accurately delinearate the reaction network.

To elucidate the complex reaction network, we employ *in situ* magic-angle spinning NMR (MAS-NMR) spectroscopy[12] to detect various stable and unstable reaction intermediates at 40 °C and 400 psi H_2. Such methods have shown exceptional advantages in understanding phase behavior and chemical transformation in mixed phase systems.[13] Similar techniques have been applied to investigate the catalytic isomerization of glucose to fructose with zeolite[14] and hydrogenolysis/hydrogenation of lignin model compounds with supported metal nanoparticles.[12]

The obtained kinetic information of molecule has been utilized to unravel the high selectivity in the PTHQ synthesis as observed for the Pd@UiO-66 catalyst.

Results and discussion

Production of PTHQ with bifunctional Pd@UiO-66

The Claisen-Schmidt condensation between NBA and ACP was carried out with three different MOFs, including UiO-66(Zr), HKUST(Cu), and MIL-101(Cr). The powder X-ray diffraction patterns of the MOF materials are shown in Figures S1-S4. Metal−organic frameworks (MOFs) have attracted great interests as Lewis acid catalyst.[15] Other active sites can be introduced by modification of the organic linkers or the impregnation of metal nanoparticles.[16] Therefore, the co-existence of different catalytic active sites can enable two or more sequential reactions. The possible formation of reactive intermediates can be converted readily by eliminating unnecessary separation and purification, and thus increase reaction efficiency and atom economy.[17]

One extra equivalent of ACP was introduced to ensure a full conversion of NBA because residual NBA may undergo more side reactions, causing complication of the reaction analysis. UiO-66 shows the highest catalytic activities on the Claisen-Schmidt condensation reaction at 100 °C achieving full conversion in 3 h, Figure 1. Such activity is owing to the combined efforts of Lewis acidic Zr with missing ligand and Brønsted site by the μ_3-OH[18] in the SBU. The strong Lewis acidity has been demonstrated in the Meerwein-Ponndorf-Verley (MPV) reduction of prenol and furfural.[19] MIL-101 with coordination-unsaturated Cr site shows only a 8% conversion in 3 h, which is much less active compared to UiO-66. HKUST-1 is also Lewis acidic but inefficient in promoting the condensation reaction, although found active in catalyzing the Friedländer reaction for the synthesis of quinoline.[20]

Furthermore, an amphoteric catalyst (UiO-66-NH_2-m) was prepared by substituting 50 mol% of the linker in UiO-66 (benzene-1,4-dicarboxylic acid) with 2-aminobenzene-1,4-dicarboxylic acid. The difference between UiO-66-NH_2-m and UiO-66 was not obvious, with a slight decrease in reaction rate. Hajek and coworkers also found that functionalization of UiO-66 with amino group only have a marginal effect on the cross-aldol reaction of benzaldehyde and heptanal.[15b] Therefore, UiO-66 is chosen as the support for Pd NPs.

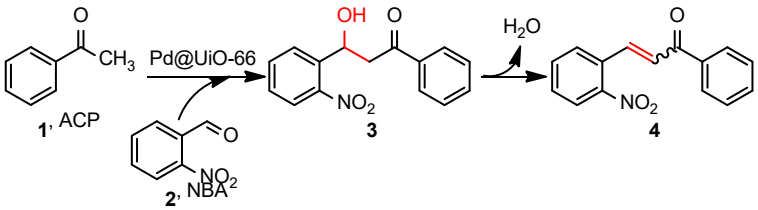

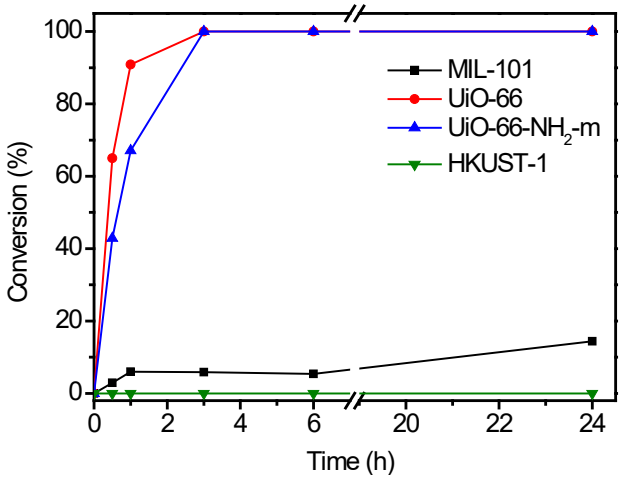

Figure 1. Conversion of NBA versus time for the MOF-catalyzed Claisen-Schmidt condensation reaction. Reaction conditions: NBA (0.2 mmol), ACP (0.4 mmol), catalyst (25 mol% in terms of metal center, calculated in Table S1), toluene (1 mL), 100 °C.

Pd@UiO-66 was synthesized via a wetness impregnation method.[16a] The powder X-ray diffraction (PXRD) patterns indicated that the UiO-66 support and Pd@UiO-66 match with the simulated pattern of the MOF itself (Figure S1a), indicating the MOF structure remained unperturbed after loading of Pd NPs (2 wt%). Besides, the Brunauer–Emmett–Teller (BET) surface area of UiO-66 before and after loading Pd is 1799 and 1528 $m^2 \cdot g^{-1}$, respectively (Figure S5 and Table S2). The micropore volume of UiO-66 decreased slightly from 0.50 to 0.46 $cm^3 \cdot g^{-1}$. No X-ray diffraction peaks were detected for Pd metal, possibly due to the small sizes and low loading of the NPs. As shown in the TEM images, the Pd NPs are dispersed uniformly on MOF with the average diameter of 4.2 ± 0.7 nm (Figure S1b). The catalytic activity in the Claisen-Schmidt condensation reaction is unperturbed with the presence of Pd, Figure S6.

Next, Pd@UiO-66 was examined as a bifunctional catalyst for the hydrogenation of ***4*** to PHTQ. The reductive cyclization of *ortho*-nitrochalcone ***4***, isolated from the previous Claisen-Schmidt condensation, was completed in 5 h with >98% selectivity to PTHQ at 40°C under 400 psi H_2 (Figure 2a). Even with ambient-pressure H_2, the full conversion of 4 is reached in 7 h at 50°C (Figure 2b). Sequential synthesis of PTHQ from NBA and ACP was successfully achieved and is discussed in a latter session. Under both conditions, PQ is formed (Figures S7 and S8), while PQ cannot be formed directly from ***4***, which is dominantly formed as the trans isomer, as confirmed by the large $^3J_{H\text{-}H}$ coupling constant (15.5 Hz), Figure S9. Besides, under similar conditions, reduction of PQ is significantly slower compared to ***4***.

Figure 2. Pd@UiO-66 catalyzed hydrogenation reaction of different substrates at (a) 40°C, 400 psi H_2, (b)50°C, atmospheric H_2. Reaction conditions: substrate (0.2 mmol), 2% Pd@UiO-66 (5 mg, ~0.5 mmol% Pd), solvent toluene (2 mL). Conversions were calculated based on analysis of GC-MS results.

All hydrogenation results suggest that the PQ is formed as a side product but rather than a key intermediate towards the formation of PHTQ. Previous works by Crabtree[6a] and Soós[6e] mostly

focused on the spectroscopic and DFT studies of reduction of PQ to PTHQ using homogeneous catalysts. However, little mechanistic information on the tetrahydroquinoline ring formation have been reported yet, most likely due to the complexity of the molecular transformation.

Mechanistic study with in situ MAS-NMR

To unveil the reductive-cyclization reaction mechanism of the PTHQ production, *in situ* MAS-NMR study was carried out in two steps. A customized MAS rotor was used to withhold vapor pressure and added gas (H_2) at elevated temperatures. In the 1st step, the Claisen-Schmidt condensation was conducted under air. The rotor was loaded with ACP and NBA (0.83 eqv) in toluene. The ACP was labelled at both α and β with ^{13}C, allowing fast tracking of molecular evolution with ^{13}C NMR. Therefore, intermediates and products can be detected as two doublets due to $^{1}J_{CC}$ while the non-labeled positions remain invisible. The Claisen-Schmidt condensation was monitored at 80 °C with the α and β carbons of ACP identified as doublets at 194.1 and 23.9 ppm, respectively (Figure 3a). These two resonances started to decrease in intensity with two new doublets at 187.0 and 126.1 ppm, which are assigned to α and β carbons of dehydrated aldol product ***4***, respectively, in Figure 3a and S10.

While there are no traces of β-hydroxyketone detected, the aldol product ***3*** has been observed when lowering the reaction temperature to 60 °C, Figure S11. The α and β carbons of ***3*** show up at 197.1 and 45.0 ppm, respectively. In ca. 4 hour, the maximal concentration of ***3*** was reached, which is about 5% of the initial ACP concentration, before complete disappearance after 11 h. No aldol products were observed between two acetophenone molecules at both tested temperatures. The concentration profiles of ACP and ***4*** were extracted from the NMR arrays at 80 °C (Figure 3a). At 12 h, the yield of ***4*** is 80 % based on ACP and the selectivity is >99%. Analysis of the data with 2nd-order rate equations yielded the curvefits shown in Figure 3b. The 2nd-order rate constants extracted from ACP and compound ***4*** are almost the same, XX and XX, respectively.

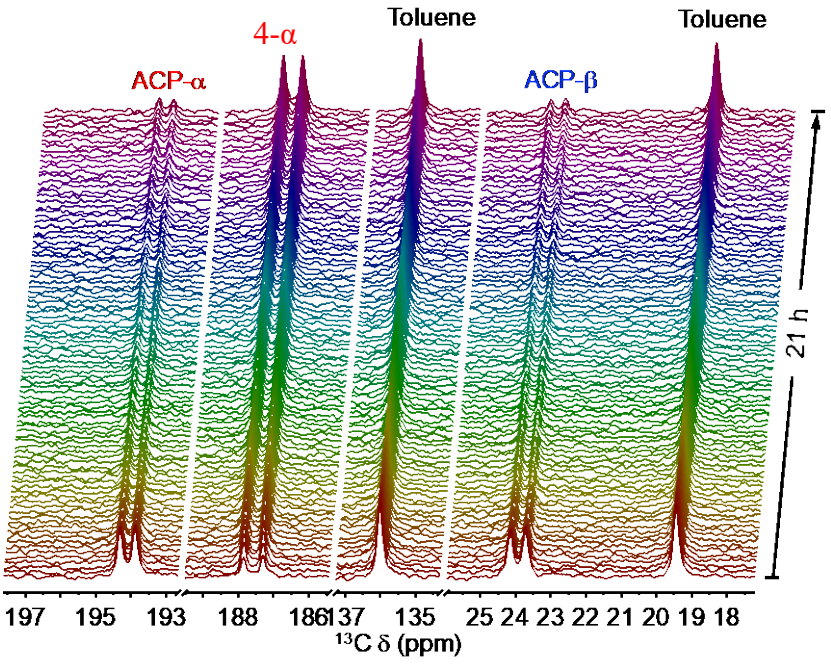

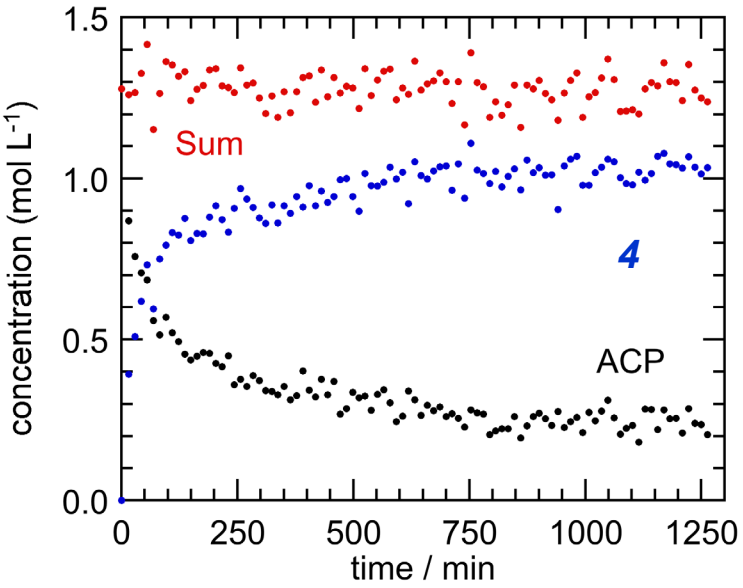

Figure 3. Direct polarization ^{13}C MAS-NMR spectra and kinetics, recorded during Claisen-Schmidt condensation reaction of acetophenone (ACP) with 2-nitrobenzylaldehyde (NBA) at 80 °C. The 5 mm NMR rotor was loaded with ACP-α,β-$^{13}C_2$ (7.81 mg, 63.9 μmol), NBA (8.04 mg, 53.3 μmol), 1%Pd@UiO-66 (1 mg), and 50 μL toluene. MAS rate: 5 kHz.

After the Claisen-Schmidt condensation reaction, the rotor was recovered from the spectrometer and charged with 400 psi H_2 when the solution and catalyst were still kept inside. After re-insertion to the spectrometer, the rotor was heated to 40 °C and maintained for 22 h. Higher pressure of H_2 gas (400 psi instead of 100 psi) was applied in the *operando* study to ensure large excess of H_2 (10 times of ***4*** by mol). Lower temperature (40 instead of 80 °C) is also applied to slow down the reaction to better probe the intrinsic property of catalyst and detect reactive intermediates.

Both resonances of ***4*** disappeared after the first three spectra (in 40 min) with the appearance of several sets of doublets. Two new resonances at 187.2 and 119.6 ppm instantly appeared in the first spectrum and disappeared in the first 2 hours, which can be assigned to the α and β carbon of compound 7, the reduction product of ***4*** only at the nitro group. The complete scheme of the reductive cyclization is demonstrated in Scheme 2. The formation of ***7*** is also confirmed with UPLC-UV-MS showing a m/z = 224.0 (+ H^+) in the mass spectrum (Figures S12 and S13). A resonance appeared at 121.0 ppm although the pairing one cannot be identified, most likely due to peak overlap. This peak is less likely to be ***11***, the hydrogenation product of PQ, since the concentration build-up of PQ happens posterior to the disappearance of this unassigned peak. A possible assignment to the condensation product of ***9*** and acetophenone, which has been observed by GC-MS (Figure S14).

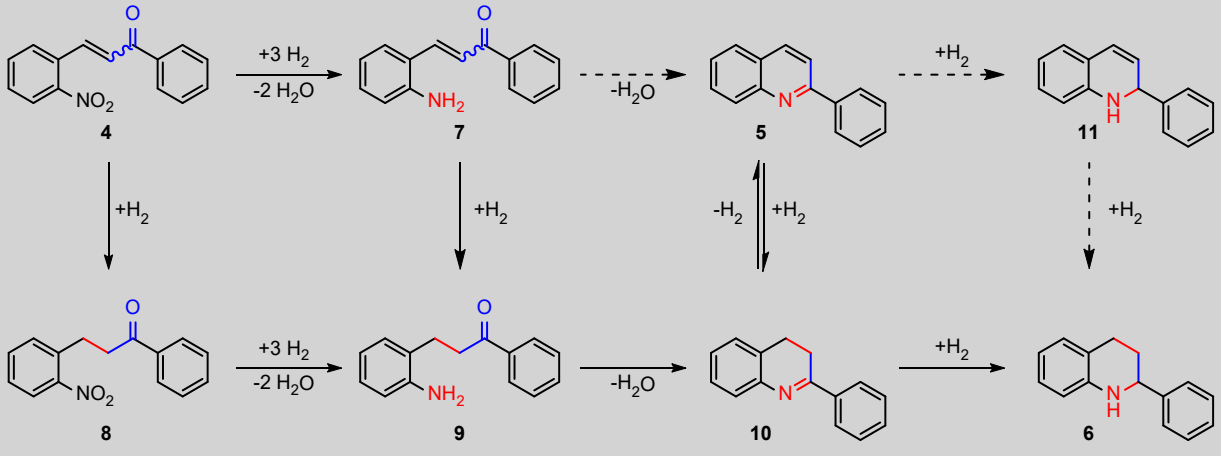

Scheme 2 Plausible intermediates in the Pd@UiO-66 catalyzed hydrogenation of ***4*** for the synthesis of PTHQ.

The two doublets at 195.3 and 37.5 ppm are assigned to α and β carbons of ***8***, the C=C bond reduction product of ***4***. The chemical shifts are verified by an authentic sample of ***8*** (Figure S15). The presence of ***8*** in the reaction mixture is further confirmed by UPLC-UV-MS, giving a peak with m/z = 256.1 (+ H^+) in the mass spectrum (Figure S16).

Compound ***9***, the further hydrogenation intermediate of either ***7*** or ***8***, cannot be found in the spectra, nor detected by neither GC-MS or UPLC-UV-MS. The absence of ***9*** is possibly due to its low concentration as it readily cyclizes. If it is present, the NMR signals may not be well separated from those of ***8***. But the detection of ***8***, can indirectly prove the existence of ***9*** as a short-lived key intermediate.

PQ and PTHQ are observed in array of MAS- NMR spectra as expected products, also detected by UPLC-UV-MS (Figures S17 and S18). The resonances at 155.3 and 116.8 ppm are assigned to PQ-α and PQ-β carbons, respectively. The resonances at 54.7 and 29.7 ppm are assigned to PTHQ-α and PTHQ-β carbons, respectively.

There is another set of two pronounced doublets in the spectra at 163.3 and 22.3 ppm. The only possible assignment for these two resonances are compound ***10***, which agrees with the literature results on an isolated sample.[21] Compound ***10*** is readily subject to decomposition under heating or oxidation to PQ, which may not be stable even for at-line analysis. Therefore, ***10*** cannot be detected by traditional techniques, including TLC (Figure S19), GC-MS (high injector temperature at 300 °C) or UPLC-UV-MS (column temperature: xx °C and MS probe temperature at 600 °C), although the maximal concentration of compound ***10*** is as high as 0.44 mol L^{-1} at 4 h before its complete conversion. This clearly showed the unique capability of *operando* MAS-NMR spectroscopy to detect and quantify reactive intermediates to understand complexed reaction networks whereas *ex situ* methods only provide insufficient and misleading results in interpreting reaction pathway.

Other work indicates the possible formation of three partially hydrogenated intermediates (1,2-, 2,3-, and 3,4-dihydroquinolines) towards the production of tetrahydroquinolines. 2-phenyl-1,2-dihydroquinolines was prepared *via* the addition of organometallic reagents to quinoline,[22] which

can be subsequently reduced to tetrahydroquinolines in the presence of Na/EtOH. The direct identification of ***10*** was only once reported but not quantified during the direct hydrogenation of quinones catalyzed by homogeneous Ru complex, using ESI-HRMS.[21]

The concentration profiles of **4**+**7**+**8**, **10**, PQ, and PTHQ (using resonances of corresponding α carbons) are shown in Figure 5. However, the maximal concentration of PQ, 0.10 mol L^{-1} (yield: 8 %) was reached at 7 h. The kinetics from *operando* MAS-NMR strongly suggests that PTHQ is mostly derived from **9** but not from PQ.

To better benchmark the rates of hydrogenation, experiments starting with **8** compared with **4** and **5** were conducted under two conditions of 40 °C with 400 psi H_2 (Figures 2a and S7) and at 50 °C with ambient H_2 (Figures 2b and S8). Under both conditions, the hydrogenation of compound **4** is the fastest, because **4** can be converted to PTHQ through two subsequent pathways (to **7** and **8**). PQ is the most difficult to be reduced to tetrahydroquinoline under the same reaction conditions, which further verified that PTHQ was not mostly produced from PQ. Therefore, the PQ is yielded mostly due to the Pd@UiO-66 catalyzed equilibrium with ***10*** in the presence of H_2. Similar dehydration reactions have been reported for Pd based catalysts for applications like reversible hydrogen storage.[23]

The residual ACP decreases by half in concentration after 21 h, which is due to its partial hydrogenation to benzyl alcohol. Intermediates **7**, **8**, and **9** can also be subject to reduction to form benzyl alcohol derivatives, resulting in the formation of three doublets at 71.5, 68.4, and 65.8 ppm, in Figure S20.

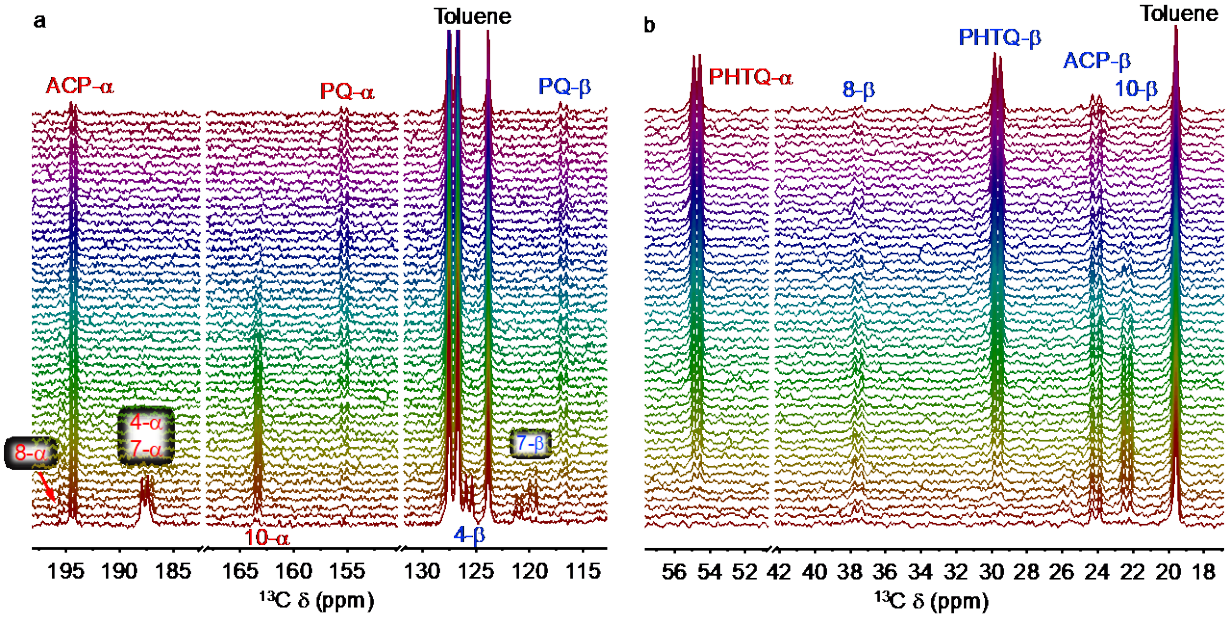

Figure 4. *In situ* array of direct polarization ^{13}C MAS-NMR spectra, recorded during hydro-cyclization of ***4*** to form PHTQ at 40 °C. The 5 mm NMR rotor, containing the end solution after aldol condensation was pressurized with 400 psi H_2 at 22 °C. MAS rate: 5 kHz.

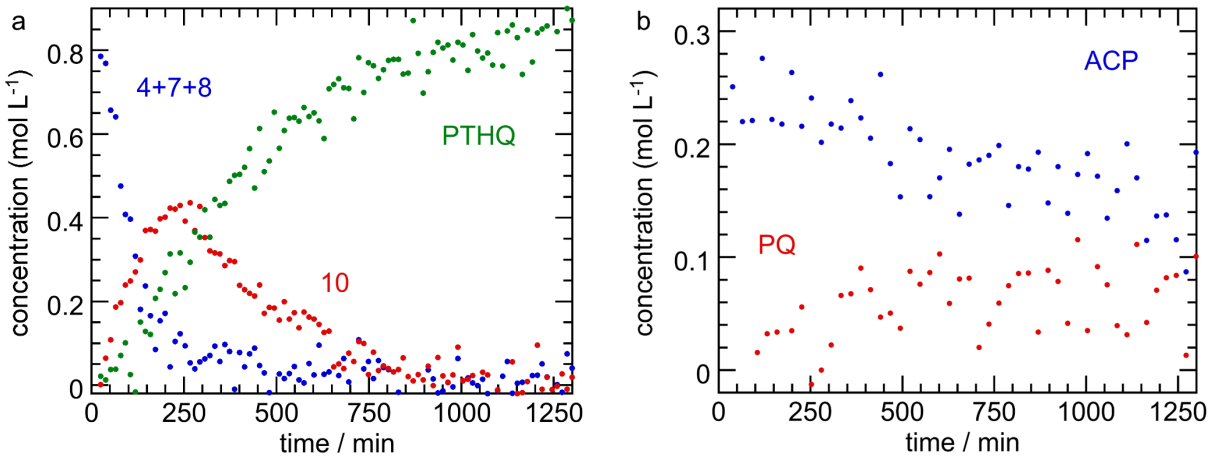

Figure 5. Concentration profile of hydrocyclization of ***4***, extracted from *in situ* MAS-NMR at 40 °C. The 5 mm NMR rotor, containing the end solution after aldol condensation was pressurized with 400 psi H_2 at 22 °C. MAS rate: 5 kHz.

Reaction optimization and expansion of substrates

The reactor after the Claisen-Schmidt condensation (step 1, 5 h at 100 °C) was directly charged with H_2 for cyclization (step 2) without any additional treatment. Under 400 psi H_2, the reductive cyclization of ***4*** was completed in 5 h with >98% selectivity to PTHQ at 80 °C instead of 40 °C (Table 1, entry 1). At 80 °C but with 100 psi, similar yield of PTHQ (86%) is achieved in 19 h. The reaction can even proceed with ambient-pressure H_2, although the yield toward PTHQ decreased slightly to 78% (Table 1, entry 3) in 19 h. Hence, the optimized reaction conditions are 0.1 mmol 2-nitrobenzaldehyde, 0.2 mmol acetophenone and 5 mg of 2% Pd@UiO-66 in 1 mL of toluene reacted at 80°C under air for 5 h, then hydrogenated under 100 psi of H_2 at 80°C for 19 h.

Table 1 Pd@UiO-66 catalyzed one-pot synthesis of PTHQ.[a]

entry	H_2 (psi)	time (h)	yield (%)[b]	
			PTHQ	**PQ**
1	400	8	90	<1
2	100	19	86	2
3	14.5	19	78	5
4[c]	100	19	54	7

[a] Reaction conditions: step 1: NBA (0.1 mmol), ACP (0.2 mmol), 2 wt% Pd@UiO-66 (5 mg), toluene (1 mL), 80 °C for 5 h; step 2: at 80 °C with H_2 of different pressure. [b] Yield calculated by GC with mesitylene as the internal standard. [c] With 1 wt% Pd@UiO-66.

After establishing the optimal reaction conditions, we further explored the scope of Pd@UiO-66 catalyzed tandem reactions for the synthesis of PTHQs with different substitutes (Scheme 3). The reaction went smoothly with both electron-withdrawing (**1b**, **1c**) and electron-donating (**1d**) substituents on acetophenone. With 4-nitroacetophenone as substrate, the nitro group was reduced

to amine (**6c**) under the standard reaction conditions. Electron-withdrawing substitutes on *ortho*-nitrobenzaldehyde (**2e**-**2g**) have minor effect on the yield of THQs, but the electron-donating group decreased the reactivity of *ortho*-nitrobenzaldehyde (**2h**) and higher H_2 pressure is needed to improve the yield of **6h**. The isolated yield is lower than 100%, possibly due to the adsorption of PTHQs on UiO-66.

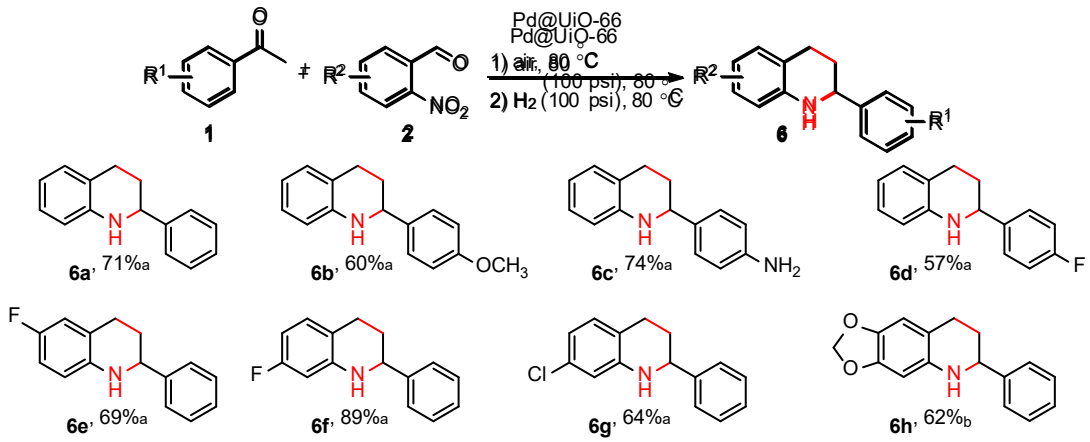

Scheme 3 Pd@UiO-66 catalyzed tandem reaction for the synthesis of tetrahydroquinolines, showing isolated yields. [a]Reaction conditions: 2-nitrobenzaldehydes (0.2 mmol), acetophenone (1.2 equiv.), 2 wt% Pd@UiO-66 (10 mg), toluene (1 mL); step (1) 80 °C, 5 h and step (2) 100 psi H_2, 80 °C, 19 h. [b]2 wt% Pd@UiO-66 (20 mg); step (1) 80 °C, 10 h and step (2) H_2 (400 psi), 80 °C, 38 h.

Conclusion

An acidic MOF with supported Pd NPs, Pd@UiO-66, was synthesized for the one-pot synthesis of PTHQ. The acidic sites of UiO-66 was efficient in catalyzing the Claisen-Schmidt condensation between NBA and ACP (100% conversion of NBAs), while the Pd nanoparticles were active toward the reductive cyclization of *ortho*-nitrochalcone. PTHQs were formed in one-pot, up to 99% selectivity, without any additional separation of the reaction intermediate. *Operando* MAS-NMR spectroscopy was employed to identify reactive intermediates and their kinetics for mechanistic investigation. Plausible reaction route was proposed, with *in situ* observed 2-phenyl-3,4-dihydroquinoline as the key intermediate.

Experimental

Chemical The following chemicals were obtained from commercial suppliers and used as received: 2-nitrobenzaldehyde (Acros Organics, 99+%), acetophenone (Fisher Scientific, ACS grade), acetophenone-α,β-$^{13}C_2$ (Aldrich, 99 atom % ^{13}C), benzene-1,4-dicarboxylic acid (BDC, Aldrich, 98%) zirconium (IV) chloride (Alfa Aesar, 98%), *N*,*N*-dimethylformamide (Macron), toluene (Fisher Scientific, reagent grade), dichloromethane (Fisher Scientific), ethanol (EtOH, 200 PROOF), palladium (II) acetate (Oakwood Chemical, 99%), potassium tetrachloroplatinate (II) (Acros Organics, 99.9+%), hydrochloric acid (Fisher Scientific, TraceMetal grade), and nitric acid (Fisher Scientific, TraceMetal grade).

3-(2-nitrophenyl)-1-phenylpropan-1-one (***8***) was synthesized according to a method reported in literature.[24] The 2-nitrocinnamaldehyde (3.0 mmol, 1.0 equiv), phenylboronic acid (3.3 mmol, 1.1 equiv), $Rh_2(OAc)_4$ (0.03 mmol, 1.0 mol %), $[(t\text{-}Bu)_3PH]BF_4$ (0.075 mmol, 2.5 mol%), K_2CO_3 (0.3 mmol, 10.0 mol%) and toluene/H_2O (v/v = 3/1, 12 mL) were added into a Schlenk tube, the air in the tube was replaced by N_2 *via* three freeze-thaw-pump procedures. Then, the mixture was warmed up to room temperature and then heated to 90 °C and kept at this temperature for 4 h. The reaction mixture was extracted with ethyl acetate (3 × 5 mL) and washed with water (2 × 10 mL). The organic layer was separated and dried over Mg_2SO_4. The solvent was removed by rotary evaporation, the dark solid was purified by flash column chromatography, with ethyl acetate/hexane as the eluent, the product is light yellow solid. Yield: 86%.

Synthesis of UiO-66 *and* ***Pd@UiO-66*** UiO-66 was synthesized and purified according to a method described in literature.[25] Typically, $ZrCl_4$ (125 mg, 0.54 mmol), hydrochloric acid (1 mL) and DMF (5 mL) were mixed and sonicated for 20 min. BDC (123 mg, 0.75 mmol) and DMF (10 mL) was added to the clear solution and sonicated for another 20 min to make it dissolved. After heated at 80 °C for 16 h, the resulted white solid was separated by centrifugation and washed with DMF (3×20 mL) and EtOH (3×20 mL) thoroughly. The solid was activated by heating at 120 °C for 24 h before catalysis.

To 100 mg of UiO-66 was added 5 mL of dichloromethane (DCM), the mixture was sonicated for 1 h to disperse the solid homogeneously. 5 mL of DCM containing 4.2 mg of palladium acetate was added to the above suspension under vigorous stirring. After stirring at room temperature for 24 h, the solid was separated by centrifugation and washed with DCM for 5 times to remove the free palladium salts completely. The solid was dried under vacuum and reduced under 10% H_2/Ar with a flow rate of 50 mL/min at 200 °C for 2 h.

Nitrogen physisorption study of all materials were used to measure the BET surface area on a Micromeritics 3Flex instrument at 77 K after degassing at 120 °C for 24 h (<20 mtorr). The powder X-ray diffraction (XRD) patterns were obtained on STOE Stadi P powder diffractometer using Cu Kα radiation (40 kV, 40 mA, λ = 0.1541 nm). ICP-MS was conducted on X Series II, Thermo Scientific instrument to determine the loading of palladium. The sample was calcinated at 500 °C for 5 h and added aqua regia and boiling it till all solid dissolved completely.

Catalytic reactions Generally, 2-nitrobenzaldehyde (0.1 mmol), acetophenone (2 equiv.), Pd@UiO-66 (5 mg), mesitylene (3 μL, as internal standard) and toluene (1 mL) was stirred at 80 °C for 5 h. Then, the mixture was hydrogenated under 100 psi of H_2 for 19 h.

The conversion and selectivity of the product were determined by GC. The product was analyzed using Agilent 5975 gas chromatograph with a flame ionization detector (GC-FID) and Agilent 6890N gas chromatography-mass dectector (GC-MS). Both are equipped with an HP-5MS capillary column (30 m × 0.25 mm × 0.25 μm). HPLC separation was conducted on an Agilent 1100 series HPLC (COSMOSIL 5C18-MS-II, 4.6 mm I.D. × 250mm). The MS detector is Bruker amaZon ETD instrument, using a ESI/APCI io source with a dry gas flow rate at 8 L/min at 220 °C. The MS capillary tube pressure is 4500 V. ^{1}H NMR and ^{13}C NMR spectra were measured on a Bruker Avance III spectrometer (9.4 T) or Agilent DirectDrive2 spectrometer (14.1 T). TOF-MS spectra were collected using a Waters GCT Premier instrument.

In situ MAS-NMR spectroscopy. Magic-angle-spinning (MAS) NMR experiments were performed on an Agilent DD2 400 MHz (9.4 T) spectrometer equipped with a 5-mm triple-resonance Chemagnetics probe, operating at a MAS rate of 5 kHz. External calibration of the spectrometer temperature setting was achieved by ethylene glycol.[26] ^{13}C chemical shifts were referenced to TMS via a secondary standard, adamantane (37.48 ppm).[27]In direct polarization (DP) ^{13}C MAS-NMR experiments, a 50 kHz ^{1}H decoupling field was employed, with an acquisition time of 327 ms. The ^{13}C spectral width was 50 kHz, and 64k data points were acquired per transient, using a relaxation delay of 100 s to ensure quantitative analysis. Each transient spectrum was acquired by averaging 8 scans, unless specified otherwise. Spectra were collected starting when the probe reached its set temperature, ca. 5-10 min after heating of the rotor commenced.

For the Claisen-Schmidt condensation reaction, a customized 5 mm ZrO_2 rotor (*WHiMS* rotor, Revolution NMR) was loaded with acetophenone-α,β-$^{13}C_2$ (7.81 mg, 63.9 μmol), 2-nitrobenzaldehyde (8.04 mg, 53.3 μmol), 1 wt% Pd@UiO-66 (1.0 mg), and 50 μL toluene under air. For the reductive-cyclization reaction, the rotor with the catalyst and the end solution after Claisen-Schmidt condensation was pressurized with 400 psi H_2 at 22 °C. The spectrum arrays were collected at 80 and 40 °C, respectively.

Acknowledgement

We thank the support from Iowa State University. L.Q. and T.K. are supported by the U.S. Department of Energy (DOE), Office of Basic Energy Sciences, Division of Chemical Sciences, Geosciences, and Biosciences. The Ames Laboratory is operated for the U.S. DOE by Iowa State University under Contract No. DE-AC02-07CH11358. We are grateful for financial support from the National Key R&D Program of China (2016YFA0202900), the National Natural Science Foundation of China (21878266, 21722609). J. Chen thanks Zhejiang University for financial support. We thank Gordon J. Miller for the use of the XRD instrument.

References

[1] A. R. Katritzky, S. Rachwal, B. Rachwal, *Tetrahedron* **1996**, *52*, 15031-15070.

[2] a) R. H. Crabtree, *Energ Environ. Sci.* **2008**, *1*, 134-138; b) V. Sridharan, P. A. Suryavanshi, J. C. Menendez, *Chem. Rev.* **2011**, *111*, 7157-7259; c) J. D. Scott, R. M. Williams, *Chem. Rev.* **2002**, *102*, 1669-1730.

[3] I. Jacquemond-Collet, F. Benoit-Vical, Mustofa, V. Alexis, S. Edouard, M. Michèle, F. Isabelle, *Planta Med.* **2002**, *68*, 68-69.

[4] a) O. B. Wallace, K. S. Lauwers, S. A. Jones, J. A. Dodge, *Bioorg. Med. Chem. Lett.* **2003**, *13*, 1907-1910; b) T. A. Rano, E. Sieber-McMaster, P. D. Pelton, M. Yang, K. T. Demarest, G. H. Kuo, *Bioorg. Med. Chem. Lett.* **2009**, *19*, 2456-2460.

[5] B. Nammalwar, R. A. Bunce, *Molecules* **2014**.

[6] a) G. E. Dobereiner, A. Nova, N. D. Schley, N. Hazari, S. J. Miller, O. Eisenstein, R. H. Crabtree, *J. Am. Chem. Soc.* **2011**, *133*, 7547-7562; b) M. Yan, T. Jin, Q. Chen, H. E. Ho, T. Fujita, L.-Y. Chen, M. Bao, M.-W. Chen, N. Asao, Y. Yamamoto, *Org. Lett.* **2013**, *15*, 1484-1487; c) F. Chen, A.-E. Surkus, L. He, M.-M. Pohl, J. Radnik, C. Topf, K. Junge, M. Beller, *J. Am. Chem. Soc.* **2015**, *137*, 11718-11724; d) M. Rueping, A. P. Antonchick, T. Theissmann, *Angew. Chem., Int. Ed.* **2006**, *45*, 3683-3686; e) G. Erős, K. Nagy, H. Mehdi, I. Pápai, P. Nagy, P. Király, G. Tárkányi, T. Soós, *Chem.—Eur. J.* **2012**, *18*, 574-585; f) M. G. Manas, L. S. Sharninghausen, D. Balcells, R. H. Crabtree, *New J. Chem.* **2014**, *38*, 1694-1700; g) X. Qiao, Z. Zhang, Z. Bao, B. Su, H. Xing, Q. Yang, Q. Ren, *RSC Adv.* **2014**, *4*, 42566-42568.

[7] K.-i. Fujita, K. Yamamoto, R. Yamaguchi, *Org. Lett.* **2002**, *4*, 2691-2694.

[8] Y. Liu, J. Wei, C.-M. Che, *Chem. Commun.* **2010**, *46*, 6926-6928.

[9] S. Paria, M. Pirtsch, V. Kais, O. Reiser, *Synthesis* **2013**, *45*, 2689-2698.

[10] A. Patti, S. Pedotti, *Tetrahedron* **2010**, *66*, 5607-5611.

[11] G. R. Akien, L. Qi, I. T. Horváth, *Chem. Commun.* **2012**, *48*, 5850-5852.

[12] E. Walter, L. Qi, A. Chamas, H. Mehta, J. Sears, S. L Scott, D. Hoyt, *J. Phys. Chem. C* **2018**, *122*, 8209-8215.

[13] A. Chamas, L. Qi, H. S. Mehta, J. A. Sears, S. L. Scott, E. D. Walter, D. W. Hoyt, *Magn. Reson. Imaging* **2018**, DOI: 10.1016/j.mri.2018.1009.1026.

[14] L. Qi, R. Alamillo, W. Elliott, A. Andersen, D. Hoyt, E. Walter, K. Sung Han, N. Washton, R. M Rioux, J. A Dumesic, S. L Scott, E. Walter, Kee, S. Han, *ACS Catal.* **2017**, *7*, 3489-3500.

[15] a) Z. Hu, D. Zhao, *CrystEngComm* **2017**, *19*, 4066-4081; b) J. Hajek, M. Vandichel, B. Van de Voorde, B. Bueken, D. De Vos, M. Waroquier, V. Van Speybroeck, *J. Catal.* **2015**, *331*, 1-12; c) M. J. Katz, J. E. Mondloch, R. K. Totten, J. K. Park, S. T. Nguyen, O. K. Farha, J. T. Hupp, *Angew. Chem., Int. Ed.* **2014**, *53*, 497-501; d) C. M. Granadeiro, S. O. Ribeiro, M. Karmaoui, R. Valenca, J. C. Ribeiro, B. de Castro, L. Cunha-Silva, S. S. Balula, *Chem. Commun.* **2015**, *51*, 13818-13821.

[16] a) X. L. Li, Z. Y. Guo, C. X. Xiao, T. W. Goh, D. Tesfagaber, W. Y. Huang, *ACS Catal.* **2014**, *4*, 3490-3497; b) I. Luz, C. Rosler, K. Epp, F. X. L. I. Xamena, R. A. Fischer, *Eur. J. Inorg. Chem.* **2015**, 3904-3912; c) W. H. Dong, C. Feng, L. Zhang, N. Z. Shang, S. T. Gao, C. Wang, Z. Wang, *Catal. Lett.* **2016**, *146*, 117-125; d) K. Na, K. M. Choi, O. M. Yaghi, G. A. Somorjai, *Nano Lett.* **2014**, *14*, 5979-5983; e) Q. Yang, Q. Xu, H. L. Jiang, *Chem. Soc. Rev.* **2017**, *46*, 4774-4808; f) L. Chen, R. Luque, Y. Li, *Chem. Soc. Rev.* **2017**, *46*, 4614-4630;

g) C. Rosler, R. A. Fischer, *CrystEngComm* **2015**, *17*, 199-217; h) D. Jiang, G. Fang, Y. Tong, X. Wu, Y. Wang, D. Hong, W. Leng, Z. Liang, P. Tu, L. Liu, K. Xu, J. Ni, X. Li, *ACS Catal.* **2018**, 11973-11978.
[17] a) A. Dhakshinamoorthy, H. Garcia, *ChemSusChem* **2014**, *7*, 2392-2410; b) Y. B. Huang, J. Liang, X. S. Wang, R. Cao, *Chem. Soc. Rev.* **2017**, *46*, 126-157.
[18] a) J. Jiang, O. M. Yaghi, *Chem. Rev.* **2015**, *115*, 6966-6997; b) J. Hajek, C. Caratelli, R. Demuynck, K. De Wispelaere, L. Vanduyfhuys, M. Waroquier, V. Van Speybroeck, *Chem. Sci.* **2018**, *9*, 2723-2732.
[19] J. Hajek, B. Bueken, M. Waroquier, D. De Vos, V. Van Speybroeck, *Chemcatchem* **2017**, *9*, 2203-2210.
[20] P. M. Elena, Č. Jiří, *ChemCatChem* **2011**, *3*, 157-159.
[21] T. Wang, L.-G. Zhuo, Z. Li, F. Chen, Z. Ding, Y. He, Q.-H. Fan, J. Xiang, Z.-X. Yu, A. S. C. Chan, *J. Am. Chem. Soc.* **2011**, *133*, 9878-9891.
[22] S. W. Goldstein, P. J. Dambek, *Synthesis* **1989**, *1989*, 221-222.
[23] C. Deraedt, R. Ye, W. T. Ralston, F. D. Toste, G. A. Somorjai, *J. Am. Chem. Soc.* **2017**, *139*, 18084-18092.
[24] Z. Ma, Y. Wang, *Org. Biomol. Chem.* **2018**, *16*, 7470-7476.
[25] M. J. Katz, Z. J. Brown, Y. J. Colon, P. W. Siu, K. A. Scheidt, R. Q. Snurr, J. T. Hupp, O. K. Farha, *Chem. Commun.* **2013**, *49*, 9449-9451.
[26] R. E. Hoffman, E. D. Becker, *J. Magn. Reson.* **2005**, *176*, 87-98.
[27] C. R. Morcombe, K. W. Zilm, *J. Magn. Reson.* **2003**, *162*, 479-486.